JGR Oceans

RESEARCH ARTICLE
10.1029/2023JC019761

Rapidly Changing East Asian Marine Heatwaves Under a Warming Climate

S. Lee[1,2], M. S. Park[1], M. Kwon[3], Y. G. Park[3], Y. H. Kim[4], and N. Choi[5]

[1]Korea Ocean Satellite Center, Korea Institute of Ocean Science & Technology (KIOST), Busan, South Korea, [2]Ocean Science, University of Science and Technology, Daejeon, South Korea, [3]Ocean Circulation and Climate Research Center, KIOST, Busan, South Korea, [4]Department of Oceanography, Pukyong National University, Busan, South Korea, [5]Department of Urban and Environmental Engineering, Ulsan National Institute of Science and Technology, Ulsan, South Korea

Abstract The East Asian marginal seas (EAMS) are one of the fastest-warming ocean regions globally. This study presents the long-term trends (1982–2020) of extreme ocean warming events called "marine heatwaves" over the EAMS and examines the relationships between marine heatwave trends and mean SST warming trends. We focus on five subregions with different influences from atmospheric perturbation and ocean currents: the northern East Sea (N-ES), southern East Sea, Yellow Sea, Korea Strait (KS), and East China Sea (ECS). During the past four decades, marine heatwave duration and intensity in the EAMS have increased to approximately +4 days and +0.3°C per decade on average, respectively. In summer, the positive trend of marine heatwaves is the highest in the ECS, primarily due to the rapidly increasing mean sea surface temperature (SST). In winter, the N-ES reveals remarkably rapid increases in marine heatwave properties in the last two decades, with increasing rates of approximately 6.2 (4.9) times longer total duration (stronger intensity) than the global average changes. Beyond the impact of the rapid increase in mean SST, the N-ES marine heatwaves can be further extended due to the northward shift of the East Korea Warm Current. In general, mean SST changes are critical to the increasing trend in marine heatwave duration and intensity. This study further emphasizes that the changes in ocean circulation may expedite more rapid changes in extreme ocean events, which can produce more vulnerability in some places, such as the N-ES, to marine heatwaves under continued global warming.

Plain Language Summary Extreme warming events of the ocean occurring from several days to weeks significantly impact marine ecosystems. This study investigates the increasing trends of extremely high ocean warming, namely "marine heatwave," over East Asian marginal seas. During the past four decades, marine heatwave duration and intensity have increased to approximately +4 days and +0.3°C per decade on average, respectively. Comparing the earlier period (1982–2000) and the recent period (2001–2020), the most dramatic changes in marine heatwave properties, including frequency, duration, and intensity, occur in the northern East Sea in winter, significantly increasing 763.33% in duration. During summer, the East China Sea reveals the most significant increasing ratio of marine heatwave properties, with change rates of 227.07% in duration. Marine heatwave characteristics have a statistically increasing trend in both seasons in most regions due to global warming. Beyond the impact of the change in mean SST, we find the change in SST variance via shifting ocean current leads to the excessive trend of marine heatwaves.

Key Points:

- East Asian Marine heatwave duration and intensity have enhanced to approximately +4 days and +0.3°C per decade
- During winter, the marine heatwave duration over northern East Sea regions experiences a dramatic increase of 763.33%, much higher than the global average increase of 122.63%
- Northward ocean current variance is a significant factor in the excessive increase of marine heatwave duration, in addition to the changing mean sea surface temperature

Supporting Information:

Supporting Information may be found in the online version of this article.

Correspondence to:

M. S. Park,
mspark@kiost.ac.kr

Citation:

Lee, S., Park, M. S., Kwon, M., Park, Y. G., Kim, Y. H., & Choi, N. (2023). Rapidly changing East Asian marine heatwaves under a warming climate. *Journal of Geophysical Research: Oceans*, *128*, e2023JC019761. https://doi.org/10.1029/2023JC019761

Received 16 FEB 2023
Accepted 17 MAY 2023

1. Introduction

Sea surface temperatures (SSTs) reveal a significant warming trend in most regions of the global oceans in the 21st century due to global warming (Kennedy, 2014; Kim et al., 2011; Masson-Delmotte et al., 2021; Meehl et al., 2007; Stocker et al., 2014; Wijffels et al., 2016). Warming climate conditions are well known to exert influences on extreme weather (Stott et al., 2016). For several decades, many previous studies have improved our understanding of global warming impacts on atmospheric heatwave variabilities on both global and regional scales (Choi et al., 2020; Fischer et al., 2007; Larsen, 2003; Lee & Lee, 2016; Park & Schubert, 1997). In contrast, ocean extremes are a newly emerging topic. The global distribution and trends of ocean extremes have only recently been studied (Hobday et al., 2016; Oliver et al., 2018). Therefore, how extreme water physical and biological properties (e.g., SST, low-salinity, and phytoplankton biomass) have changed over the past decades remains uncertain.

Extreme surface ocean warming events are called "marine heatwaves," identified as abnormally high SSTs that last from several days to several months. In the last two decades, marine heatwaves have occurred across the global ocean, driven by various atmospheric and oceanic factors. During the 2003 European heatwave, the decreased wind stress and upward heat flux caused a marine heatwave in the central Mediterranean Sea (Olita et al., 2007). Marine heatwaves in 2019 in the eastern North Pacific were caused by a weakened North Pacific High and wind-driven upper ocean mixing (Amaya et al., 2020). The marine heatwaves in 2011 in western Australia (Feng et al., 2013) and in 2015/16 in southeastern Australia (Oliver et al., 2017) were induced by the intensification of the Leeuwin Current and East Australian Current, respectively. A marine heatwave has devastating impacts on ecological systems, such as coral bleaching (Hughes et al., 2017), mass mortality of aquatic living organisms (Wernberg et al., 2013), and change in local species (Wernberg et al., 2016). Considering the potential ecological and socioeconomic impacts of marine heatwaves, quantifying the trend and pattern of their properties is an urgent issue.

Recent work suggests that marine heatwaves have become more frequent and intense across the global ocean (Oliver et al., 2018). Researchers have found that from 1925 to 2016, the global average annual marine heatwave frequency and duration increased by 34% and 17%, respectively. However, the long-term trends of regional marine heatwaves in different seasons remain questionable in most regions. Particularly, East Asian marginal seas (EAMS), bordering the Asian continent and adjacent to the subtropical western Pacific Ocean, are known as one of the world's most rapidly warming ocean regions (Bao & Ren, 2014; Belkin, 2009; Lima & Wethey, 2012; Wang et al., 2016; Wu et al., 2012). Under the influence of various atmospheric and oceanic factors ranging from the western Pacific warm pool to extratropical synoptic wave systems, East Asian marine heatwaves require an in-depth approach to investigate their physical processes (Gao et al., 2020; Lee et al., 2020; Yao et al., 2020). Gao et al. (2020) focused on three consecutive marine heatwaves during 2016–2018 in terms of various factors, such as the temperature budget, shortwave radiation, ocean currents, and vertical mixing of ocean water. Lee et al. (2020) emphasized two different major modes of East Asian marine heatwave: one is associated with the transition from El Niño to La Niña conditions and the circumglobal teleconnection (CGT)-like pattern, and the other is related to the convective forcing from the subtropical western North Pacific, known as the Pacific-Japan (PJ) pattern, which modulates the interannual variability in summer-time marine heatwave durations.

Despite the recent focus on physical drivers of interannual variability (Lee et al., 2020), the seasonal differences in long-term trends of East Asian marine heatwave properties remain a question. Over the midlatitude seas, any change in marine heatwave properties in both winter and summer can significantly influence marine ecosystems (KMI, 2020). We separately investigated the trends in marine heatwave events during summer and winter. Note that there is a seasonal contrast in the major climate system in the East Asia region (Wang, 2006). Typically, southwesterly monsoonal flows and the northern Pacific subtropical high dominate in summer climate; winter atmospheric perturbations are attributed to the northerly monsoon flows, Siberian High and Aleutian Low. This study quantifies the long-term trends of marine heatwave duration, intensity, and frequency during the period of 1982–2020 while the satellite SST records are available. We focus on three questions. (a) How do summer and winter marine heatwave duration, intensity, and frequency change over the past four decades or so? (b) How does the change in mean SSTs explain the trends in marine heatwave properties? (c) In addition to global warming effects, which atmospheric and/or oceanic variances are responsible for changes in marine heatwave properties? Section 2 describes the data and methodology used for this study. Section 3 presents the results by focusing on the long-term variability in marine heatwave frequency, duration, and intensity. Section 4 discusses the possible processes that are reasonable for the notable marine heatwave changes. The final section summarizes the current findings.

2. Data and Methodology

2.1. Data

We use National Oceanic and Atmospheric Administration (NOAA) 1/4° daily Optimum Interpolation Sea Surface Temperature (OISST) High Resolution Data set Version 2 (Reynolds et al., 2007) to analyze the trends in the mean SST and marine heatwave characteristics for the period 1982–2020. The data are produced through the combination of various observations from satellite and in situ platforms (ships, buoys, and Argo floats) at 0.25° latitude × 0.25° longitude horizontal resolution.

The fifth generation of European Reanalysis (ERA5, Simmons et al., 2020) reanalysis monthly data are used to analyze the anomalous sea level pressure (SLP) and 850-hPa wind. ERA5 is produced by the Copernicus Climate

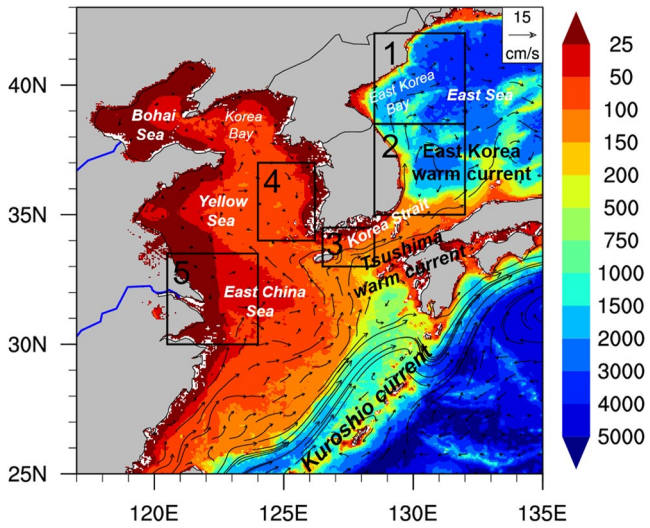

Figure 1. Bathymetry of the East Asian Marginal Seas (unit: m) using ETOPO1 (Earth topography 1 arc min) data produced by National Oceanic and Atmospheric Administration (NOAA). The box regions designate the Northern-East Sea (#1 in black box, 38.5°−42°N, 128.5°−132°E), (2) Southern-East Sea (#2, 35°−38.5°N, 128.5°−132°E), Korea Strait (#3, 33°−34.5°N, 126.5°−128.5°E), Yellow Sea (#4, 34°−37°N, 124°−126.2°E), and East China Sea (#5, 30°−33.5°N, 120.5°−124°E). The blue lines over East China indicate Yellow River (upper line) and Yangtze river (bottom line). The black arrow represents the climatology of ocean current for 1993–2012 using GLORYS.

Change Service at European Centre for Medium-Range Weather Forecasts (ECMWF) at a 0.25° latitude × 0.25° longitude horizontal resolution and 137 levels from the surface to 0.01-hPa.

The Global Ocean Reanalysis and Simulation (GLORYS) product is the Copernicus Marine Environment Monitoring Service (CMEMS) global ocean eddy-resolving reanalysis covering the altimetry for the period 1993 onward (Garric et al., 2018). The model component is a Nucleus for European Modeling of the Ocean (NEMO) driven on the surface by European Centre for Medium-Range Weather Forecasts (ECMWF) data. Along with track altimeter data (above sea level), satellite sea level temperature, sea ice concentration, in situ temperature, and salinity vertical profiles are jointly assimilated. We use the daily GLORYS data to analyze the ocean currents to 50 m depth at 0.25° latitude × 0.25° longitude horizontal resolution for data the period 1993–2020.

2.2. Marine Heatwave Detection

This study follows the methodology of Hobday et al. (2016) and Oliver et al. (2018). Using the daily OISST data, marine heatwave events at each grid are detected when the daily SST exceeds the extreme threshold, the 90th percentile SST of the 30-year daily SST values. To measure the seasonally varying 90th percentile thresholds, the daily SSTs are calculated within an 11-day window centered on the corresponding date of the year from 1982 to 2011. Next, the 31-day moving average is adjusted to smooth the 90th percentile thresholds. Based on the detected data set of marine heatwave events over 39 years, we define "frequency" as the number of marine heatwave events in each season, "duration" as the total days of marine heatwave events in each season, and "intensity" as the maximum SST anomaly relative to the climatological mean during marine heatwave events.

In this study, we define 3 months with lower SST means (January-February-March, JFM) as winter and those with higher means (July-August-September, JAS) as summer. In the climatological seasonal evolution, the cold sea waters across the EAMS during winter become warm from May. Overall, the regional sea is warmest in August and coldest in February (not shown).

To investigate the effect of global warming (mean climate change) on marine heatwave variability, the detrended SST is calculated for marine heatwave detection. Detrended SST is calculated by collecting the exact date and eliminating the mean trend using the daily OISST from 1982 to 2020. In other words, the trend of January 1 is removed by assembling SST for 39 years (1982–2020) only on January 1. Marine heatwave is detected by calculating a new threshold using the new SST data, in which the linear trend was removed.

2.3. Study Regions

The five selected ocean regions are shown in Figure 1: the northern East Sea (N-ES, #1), the southern East Sea (S-ES, #2), the Korea Strait (KS, #3), the Yellow Sea (YS, #4), and the East China Sea (ECS, #5). These five regions are distinguished by contrasting depths and different ocean currents. The East Sea (ES) is a semi-enclosed marginal sea in which warm and cold currents meet in a deep basin with a maximum depth reaching 3,800 m (Figure 1). It is divided into the N-ES and the S-ES due to the large meridional gradients in SSTs and the differences in internal ocean circulation (e.g., cold water upwelling occurring only along the coastal sea of the S-ES (Kim et al., 2014; Park & Kim, 2010)). In contrast, the YS and the ECS overlie a shallow (~100 m) and broad continental shelf. The KS is located in a path where subtropical waters and heat are transferred from the ECS to the ES along the Tsushima warm current, a branch of the Kuroshio warm current. Additionally, the East Korea warm current (EKWC), a branch of the Tsushima warm current, is the northward-flowing along the eastern coast of Korea.

Figure 2 shows the seasonal mean SST averaged from 1982 to 2011 to provide an overview of winter and summer climatology across the EAMS, together with the 90th percentile thresholds for the marine heatwave definition.

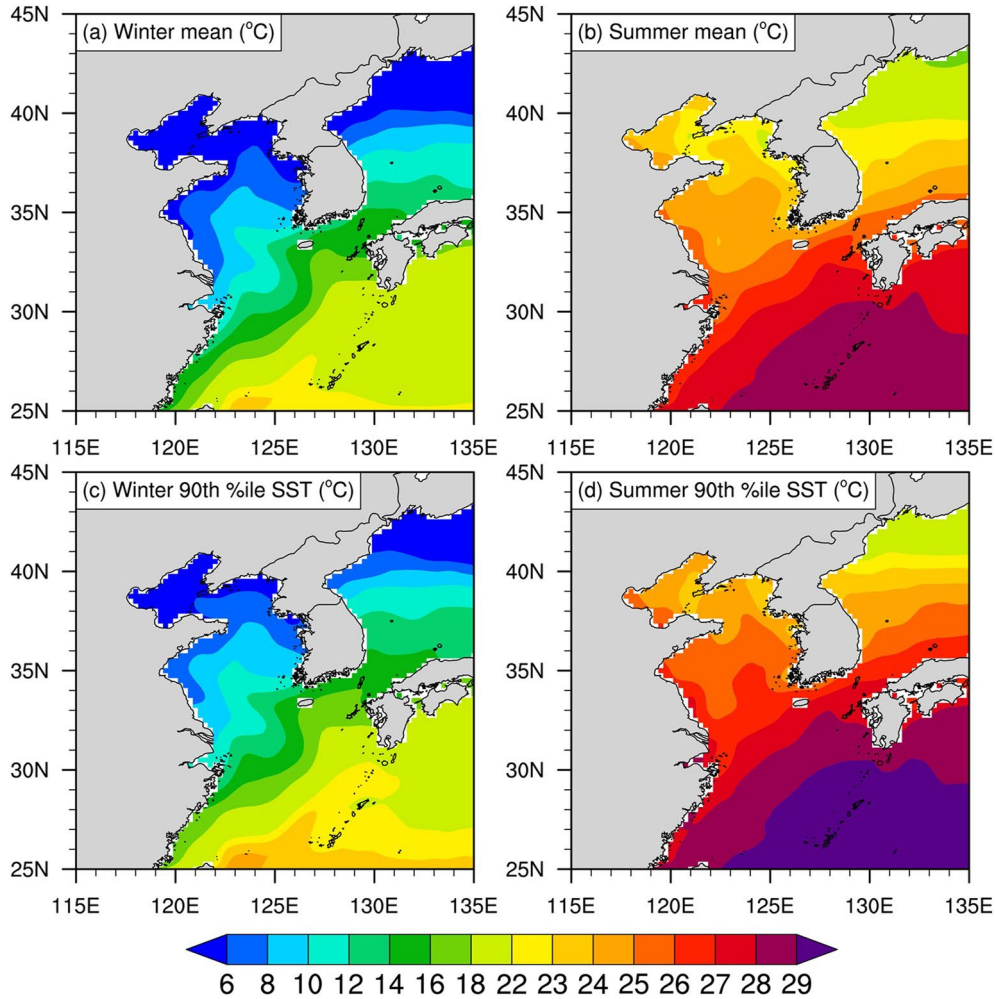

Figure 2. Seasonal mean SST (unit: °C) in (a) winter (January-February-March, JFM) and (b) summer (July-August-September, JAS) based on the OISST during the period of 1982–2011. Seasonal 90th percentile SST (°C) in (c) winter and (d) summer.

North–south gradients in seasonal mean SSTs appear during both seasons (Figures 2a and 2b). A stronger gradient occurs in winter. Since the Tsushima warm current transports subtropical water to the KS throughout the year, the SSTs in the KS are approximately 2–5°C warmer than those in the western ECS at the same latitudes. Additionally, the ocean surface of the YS with shallow depth cools (warms) quickly, revealing lower (higher) SSTs than over the ES in winter (summer) at the same latitudes due to atmospheric and oceanic changes. The 90th percentile threshold values tend to be approximately 1–2°C higher than the seasonal mean value (Figures 2c and 2d). For instance, winter marine heatwave events over the N-ES must exceed the 90th-percentile threshold of 7.4°C, which is 1.8°C above the climatological SST value of 5.6°C. That is, marine heatwave events clearly differ from slightly higher SST anomalies in that they are defined only when a threshold is exceeded.

3. Long-Term Trend of Marine Heatwaves in the EAMS

3.1. How Have Summer and Winter Mean SSTs Changed?

There is a remarkably increasing trend in SST for both the boreal winter and summer over the period of 1982–2020 (Figure 3). The winter warming trends are statistically significant (with a 95% confidence level) over most EAMS regions, except for decreased trends off the western coast of Korea and in the middle of the ECS (Figure 3a). This cooling trend over the western coast of Korea is consistent with the results reported by Lee and Park (2020). They found weakly negative trends during winter in western coastal regions of Korea from 1982 to 2018 using OISST

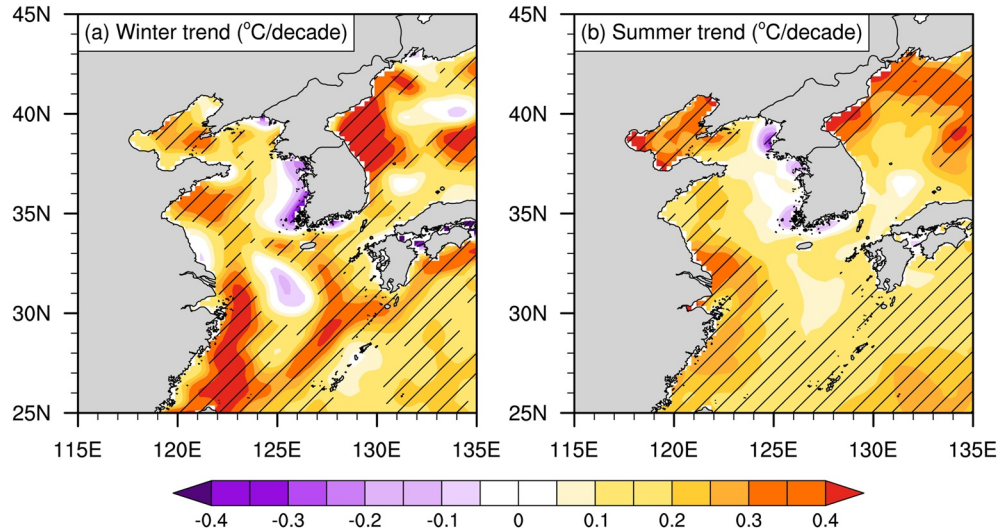

Figure 3. Long-term SST trends (unit: °C decade^{-1}) during (a) winter and (b) summer for 1982–2020. The dashed regions indicate the areas where the SST trends are significant with a 95% confidence level.

and in situ data. Previous studies (Cohen et al., 2014; Kug et al., 2015) suggested that this cooling signal is associated with cold air outbreaks in winter because of the recent warming of the Arctic Ocean and the weakening of the mid-latitude westerlies since 2000.

In summer, an increasing trend in SSTs is not statistically significant in the coastal seas around the Korean Peninsula, including the YS and KS (Figure 3b). Only the northern ES and the eastern coast of China provide significant positive trends ($p < 0.05$). Over the ECS, the increasing trends in mean SST are more rapid in winter (maximum 0.48°C decade^{-1}) than in summer (maximum 0.44°C decade^{-1}). Previous studies (Clark et al., 2020; Han & Lee, 2020; Sasaki & Umeda, 2021) have noted that the trend of SST increase in most seas is much more rapid in winter than in summer. Our result of the SST trend over the EAMS is consistent with the findings of previous studies.

Overall, the EAMS reveal the largest changes in seasonal mean SST in the ECS and the N-ES. Compared to the global change of 0.12°C decade^{-1} in winter and 0.18°C decade^{-1} in summer, the rate of increasing SST in the N-ES (ECS) region is approximately 3.1 (1.9) times higher in winter and 1.6 (1.6) times higher in summer than the global averaged trend.

3.2. Trend of Marine Heatwave Frequency, Duration, and Intensity

Over the EAMS, marine heatwaves have increasing trends in frequency, duration, and intensity from 1982 to 2020 (Figure 4 and mean spatial patterns in Figure S1 in Supporting Information S1), except for the negative trends over the seas off the western coast of Korea. In particular, stronger positive trends in winter appear in three subregions: (a) the subtropical seas from the ECS along the shoreward edge of the Kuroshio current; (b) the mid- to northern ES; and (c) the Bohai Sea. The areas with statistically significant increasing trends in marine heatwave properties correspond with those of increasing mean SST trends (Figure 3a vs. Figures 4a–4c: Figure 3b vs. Figures 4d–4f). In summer, the fastest increasing trends occur over the western YS and the northern ES (Figure 3b). The principal sea surface warming regions tend to shift approximately 5° northward in summer compared to those in winter over the ECS and the ES. Notably, the increasing trend of summer marine heatwave properties is statistically significant in the Korea Strait (Figures 4d–4f), where the seasonal mean warming is statistically insignificant (Figure 3b). Previous studies (Kim et al., 2020; Moon et al., 2019) mentioned that the KS region is affected by the freshwater from the Yangtze River. This low-salinity river discharge can increase SST due to enhancing vertical stratification by reducing vertical mixing and entrainment (Moon et al., 2019; Park et al., 2015). Although the increase in SST is insignificant, the increase in marine heatwave characteristics over the KS region can be significant due to local effects.

Now, we compare the time series of the marine heatwave properties in the five subocean regions (N-ES, S-ES, KS, YS, and ECS as in Figure 1) with the statistics in Table 1. Here, the duration and intensity rather than the frequency of marine heatwaves are selected to represent the amount of accumulated heat stress, which is more directly related

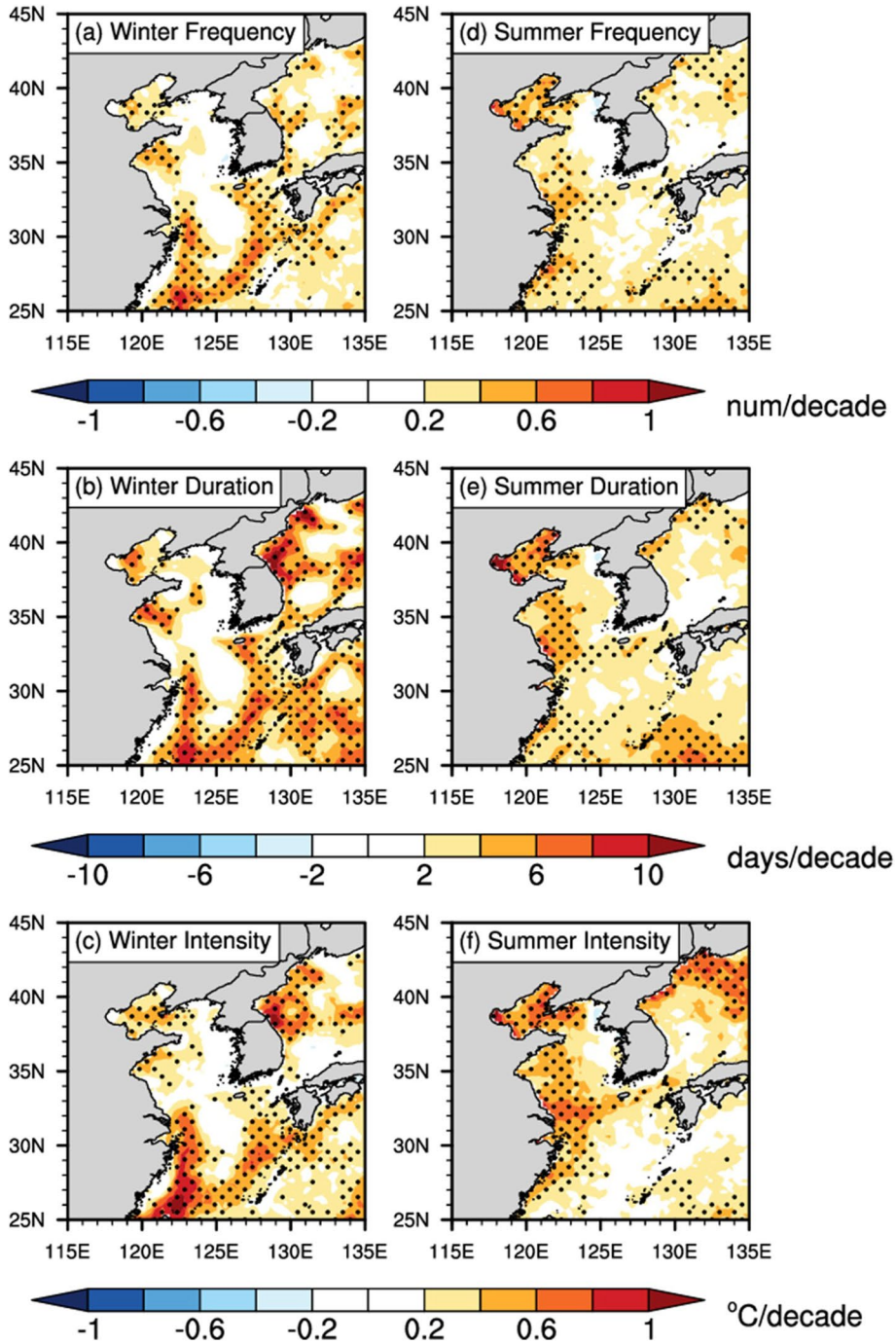

Figure 4. Trend of the marine heatwave characteristics such as (a) frequency (unit: number decade-1), (b) total duration (unit: days decade^{-1}), and (c) maximum intensity (unit: °C decade^{-1}) in boreal winter for 1982–2020. (d–f) are same as (a–c), but for boreal summer. The dotted regions indicate the areas where the trends are above the 95% confidence level.

to severe damage to the marine ecosystem. In the EAMS, marine heatwaves are longer and more robust in summer than in winter (Table 1). In winter, the marine heatwaves in the N-ES and the S-ES are longer (7–8 days) and more robust (0.8–0.9°C), while they are the shortest in the YS, with a duration of 4.58 days and an intensity of 0.61°C. The marine heatwave properties in winter have significant interannual variability across the regions, with standard deviations much higher than the mean values. In summer, the YS reveals the most prolonged marine heatwave events on average, with a duration of 9.17 days (and an intensity of 1.47°C). YS and ECS regions with shallow bottom depths exhibit average marine heatwave characteristic values 1.5 to 2 times higher in summer than in winter. A significant

Table 1
Mean and Standard Deviation (Values in Parentheses) of Marine Heatwave Duration (Unit: Days) and Intensity (Unit: °C) for the Climatological Period 1982–2011 During Winter and Summer Over the Five Study Regions

	Mean (Std)			
	Winter		Summer	
	Duration days	Intensity °C	Duration days	Intensity °C
Northern ES	8.41 (13.91)	0.94 (1.15)	8.76 (9.93)	1.67 (1.26)
Southern ES	6.88 (10.95)	0.79 (0.79)	7.76 (9.76)	1.35 (1.27)
Korea Strait	5.20 (8.34)	0.55 (0.63)	7.18 (9.26)	1.23 (1.21)
Yellow Sea	4.58 (5.71)	0.61 (0.64)	9.17 (11.01)	1.47 (1.36)
East China Sea	5.83 (7.94)	0.91 (0.98)	8.69 (9.32)	1.37 (1.18)

interannual perturbation of the marine heatwave duration, given a shallower sea depth, might be most sensitive to summertime atmospheric forcing. Also, the cold-water upwelling over summer S-ES prevents the SST from reaching the marine heatwave threshold. For this reason, YS is located at similar latitudes as S-ES, but summer marine heatwave characteristics over YS (9.17 days) are more robust than S-ES (7.76 days).

The marine heatwave duration and intensity have positive trends in all study regions, except for the YS region in winter (Figures 5a–5e, Table 2). On average, the duration and intensity of East Asian marine heatwaves in winter increased by about +4 days and +0.3°C decade^{-1}, excluding the YS region. The rapidly increasing marine heatwave regions are the N-ES and the S-ES in the winter with increasing duration (+6.15 and +4.14 days decade^{-1}, respectively) and intensity (+0.54 and +0.32°C decade^{-1}, respectively) with a 95% confidence level. The most prolonged marine heatwave duration years over the N-ES are 2020, 2017, and 2009 in recent decades. Compared to the ES region, the increasing trends in marine heatwave duration are smaller over the KS and the ECS, which increase by 3.38 and 2.65 days per decade.

In summer, all five regions show positive trends (Figures 5f–5j, Table 2). The increasing trends of marine heatwave duration are statistically significant with a 95% confidence level over the N-ES and ECS and a 90% confidence level over the KS. The most substantial change occurs in the ECS, with an increasing rate of 4.48 days decade^{-1} for duration and 0.59°C decade^{-1} for intensity. In the KS regions, the increasing trend of the mean SST is not statistically significant. As mentioned above, despite the lack of significant trends in mean SST, marine heatwave durations over the KS have significantly increasing tendencies (2.34 days decade^{-1}). There is no statistically significant trend in the mean SST or marine heatwave properties in the S-ES and YS due to large interannual variability, such as upwelling (Figures 5g and 5i, Table 2).

The peaks of atmospheric heatwaves and marine heatwaves do not always coincide. The longest and strongest marine heatwave years are summarized for each region (Table 2). In most areas, 2007, 2019, and 2020 are included in the winter marine heatwave years. In summer, the most famous summer marine heatwave years are 1994, 2001, and 2018. According to previous studies (Choi & Lee, 2019; Lee et al., 2020), the heatwave was strongest in 2018 and the second strongest in 1994 in Korea, but in 2001, the heat was not severe. This result suggests that marine heatwaves and heatwaves do not always occur simultaneously.

Lee et al. (2020) proposed two primary atmospheric and ocean modes for modulating East Asian marine heatwaves. The first spatial mode is the "basin-wide ocean warming mode" to sustain anomalous warm ocean conditions over the tropical western Pacific to East Asia from the earlier winter by El Niño-Southern Oscillation (ENSO) conditions in combination with the circumglobal teleconnection (CGT) pattern. The second mode is the "dipole mode" of SST over East Asia and the tropical western Pacific. In spring, an anomalously cold or neutral ocean surface undergoes abrupt warming over East Asia due to atmospheric high-pressure amplification in response to the enhanced tropical convection through the PJ pattern (Noh et al., 2021). We investigate the relationship between the regional time series (in Figure 5) and the two primary modes described by Lee et al. (2020). Marine heatwave durations over ES, YS, ECS, and KS have significant correlations with the first mode at a 99% confidence level (Table 3 and Figure S2 in Supporting Information S1). However, the KS and ECS regions are not statistically significantly correlated with the second mode, implying that the marine heatwave process over the KS and ECS may differ from that over other regions.

3.3. Earlier (1982–2000) Versus Recent (2001–2020) Marine Heatwaves

This subsection focuses on the difference between the earlier (1982–2000; named the "earlier period") and the recent phases (2001–2020; called the "recent period") in Figure 6. Previous studies (Jung et al., 2017; Rahman et al., 2019) reported that three recent climate regime shifts occurred in the mid-1970s, late 1980s, and late 1990s in the EAMS. Therefore, we selected 2000/2001 as the turning point, considering the most recent climate regime shift.

We calculate the increasing ratio (%) as increments in marine heatwave properties between the two periods divided by the earlier period value. The most dramatic changes occur in the N-ES in winter, which shows increases of

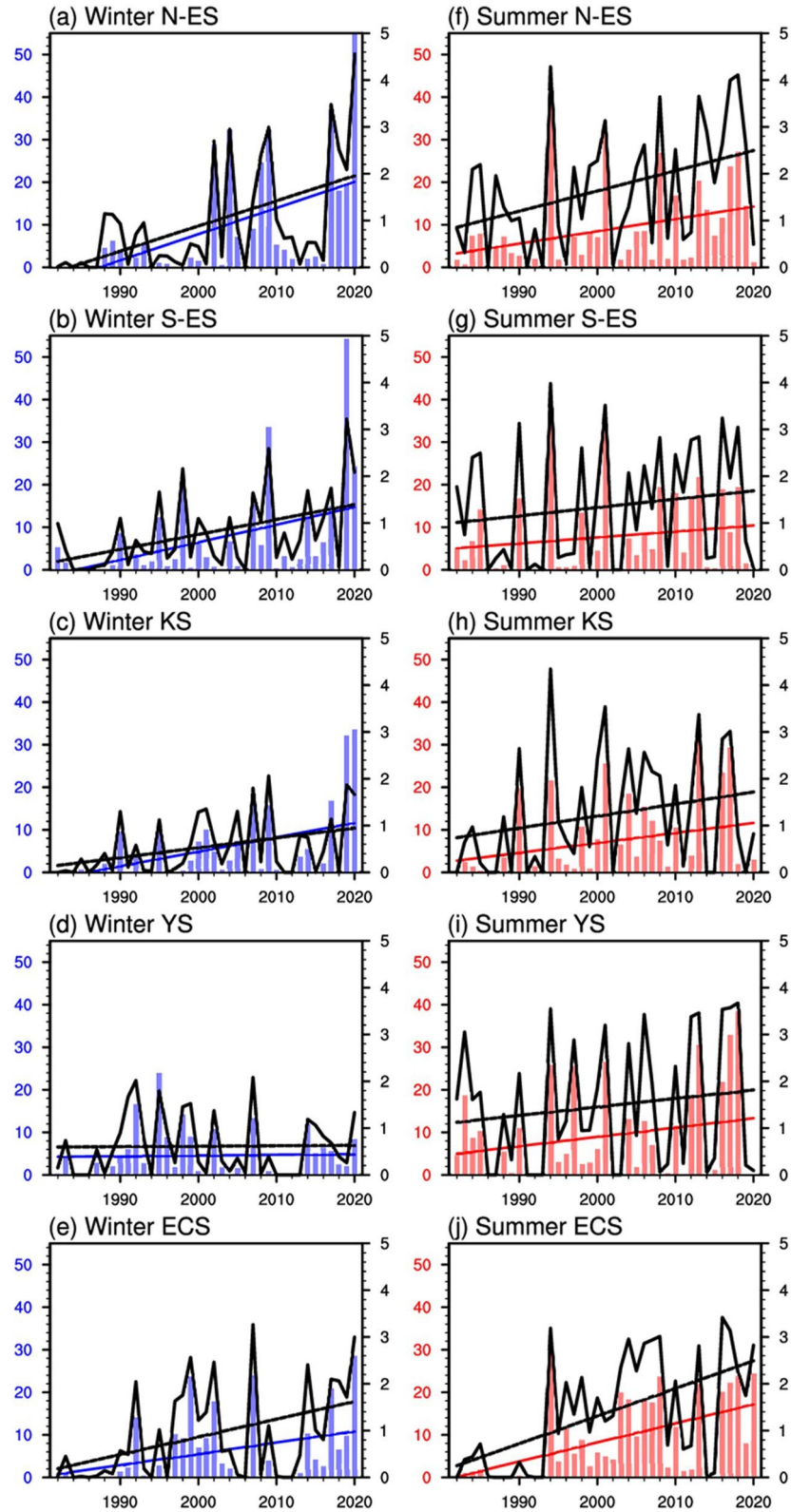

Figure 5. Time series of the regional averaged marine heatwave characteristics during winter (a–e) and summer (f–j) over study regions. Colored bar graphs indicate the marine heatwave duration (unit: days) with colored left *y*-axis value and the black line graphs mean the marine heatwave intensity (unit: °C) with black right *y*-axis value. The colored (black) solid line shows the linear trend of marine heatwave duration (intensity). Blue color means marine heatwave duration in winter and red color means marine heatwave duration in summer.

Table 2
Trend of Marine Heatwave Duration (Unit: days decade^{-1}) and Intensity (Unit: °C decade^{-1}) and From 1st to 3rd in the Year When the Marine Heatwave Was Long During Winter and Summer

	Duration trend	Longest duration year	Intensity trend
	days/decade	1st, 2nd, 3rd	°C/decade
Winter			
Northern ES	**6.15****	2020, 2017, 2004	**0.54****
Southern ES	**4.14****	2019, 2009, 2020	**0.32****
Korea Strait	**3.38****	2020, 2019, 2007	**0.21****
Yellow Sea	0.17	1995, 1992, 1998	0.01
East China Sea	**2.65****	2020, 2007, 1999	**0.38****
Summer			
Northern ES	**2.90****	1994, 2001, 2018	**0.43****
Southern ES	1.41	1994, 2001, 2013	0.18
Korea Strait	**2.34***	2013, 2017, 2001	0.26
Yellow Sea	2.19	2018, 2017, 2013	0.18
East China Sea	**4.48****	1994, 2020, 2018	**0.59****

Note. Bold numerical values are significant with a 90% (*) and 95% (**) confidence level.

306.94% in event frequency and 320.08% in intensity in the recent period versus the earlier period. In particular, the sizable increasing ratio (763.33%) in the duration at the 95% confidence level is notable. Second, marine heatwave properties increase significantly in the KS, with a change in frequency of 165.85%, duration of 261.27%, and intensity of 129.24%. The increasing rates for marine heatwaves are much larger than the global averaged rates (80.38% in frequency, 122.63% in duration, and 65.87% in intensity). In contrast, the YS reveals a decreasing change in marine heatwave properties.

In summer, the ECS reveals the most significant increasing ratio of marine heatwave properties in the recent period versus the earlier period, with change rates of 177.72% in frequency, 227.07% in duration, and 162.27% in intensity at the 95% confidence level. In the KS, the rate increases of 107.29% in frequency and 135.69% in duration are similar to the globally averaged values. In the YS, an increasing change in marine heatwave properties exists but is not statistically significant.

4. What Causes Positive Trends in Marine Heatwave Longevity and Intensity?

Regarding the overall increase in marine heatwave properties over the EAMS, the objectives of this section include (a) quantifying the roles of increasing mean SST (Section 4.1) and (b) unveiling the physical reasons behind the more rapidly increasing trend in the N-ES (Section 4.2). Central concepts for the current discussion, such as "increasing mean SST," "increasing SST variance," and "detrending mean," are precisely defined in Appendix A.

4.1. Changes to SST Mean and SST Variance

Frölicher and Laufkötter (2018) showed that a shift in mean SST causes an increasing probability of marine heatwaves. Due to the narrow distribution of SSTs, the greater increases in marine heatwaves than in atmospheric heatwaves imply that the former are more sensitive to changes in the mean climate state.

We examine the relationship between the marine heatwave duration (intensity) and the seasonal mean SST in the anomaly sense through scatterplots in Figure 7. As a result, the positive slopes indicate that an increasing mean SST induces longer and stronger marine heatwave events in both winter and summer, confirming the critical role of the mean SST change. More specifically, increasing the seasonal mean SST by 1°C leads to marine heatwave events in the EAMS that are 16 days (10 days) longer and 1.4°C (1.6°C) stronger during winter (summer). The sensitivities of the marine heatwave properties in response to increasing means are regionally different, showing dissimilar linear regression slopes in Figure 1.

Table 3
Correlation Coefficient Between Principal Component (PC) Associated Lee et al. (2020)

	Summer	
	PC1	PC2
Northern ES	**0.45****	**0.66****
Southern ES	**0.51****	**0.65****
Korea Strait	**0.67****	0.34
Yellow Sea	**0.49****	**0.67****
East China Sea	**0.39****	0.36

Note. And marine heatwave duration over study regions during 1982–2020. Bold numerical values are significant with a 99% (**) confidence level.

Next, to identify the impact of the warming ocean climate on the marine heatwave properties, the detrended daily SST is used for the analysis of marine heatwave properties (Figure 8). We recalculate the time series of marine heatwaves as described in Appendix A. In comparison with the original time series (Figure 5), the detrended mean results in the disappearance of the positive slopes in most regions (Figure 8). In the ECS, marine heatwave properties have a statistically increasing tendency in winter and summer (Figures 3 and 5); however, the recalculated marine heatwave property time series do not have statistically significant increasing trends (Figures 8e and 8j). The ECS is a typical region where ocean warming primarily contributes to extending and strengthening marine heatwave events over approximately four decades.

In contrast, the trends of marine heatwave properties remain positive over the N-ES in winter even if the linear trend is removed (Figures 8a and Table 4).

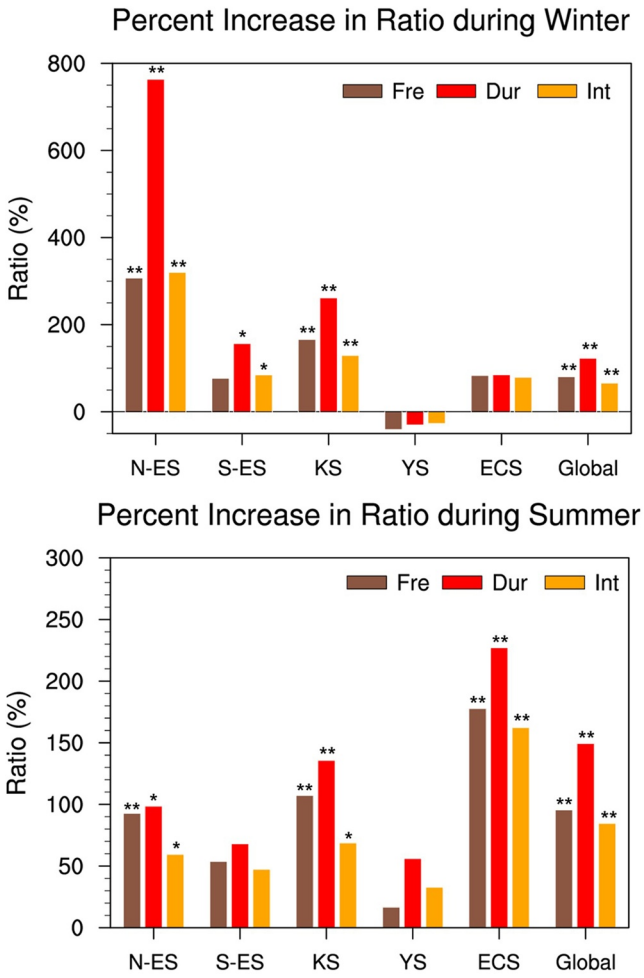

Figure 6. Percent increase in ratio of marine heatwave characteristics (Fre: Frequency in brown bar, Dur: Duration in red bar, Int: Intensity in yellow bar) during 2001–2020 compared to 1982–2000 in winter (top panel) and summer (bottom panel). Global values indicate the average in the global ocean regions. Marks above the bars indicate the significant value with a 90% (*) and 95% (**) confidence level.

To understand the excessive trend in marine heatwaves beyond the impact of the changing mean trend, Figure 9 compares the probability distribution function of SSTs between the earlier and recent periods. Interestingly, we find dramatic changes in SST variance from the earlier to the recent period, showing a 0.97 to 1.69 increase in SST variance in Figure 9c (with a 95% confidence level of the *F*-test). This recently increasing winter SST variance (Figure 9c) is in contrast to that in summer (Figure 9d). Accordingly, the changing SST variance (Figure 9c) leads to the excessive trend of winter marine heatwaves over the N-ES even after detrending the mean (Figure 9a). This result corresponds with that of Oliver (2019), who emphasized the importance of SST variance on marine heatwave exposure, particularly over the highly variable mid-latitude western boundary current regions, including the EAMS.

4.2. Physical Driver of Excessive N-ES Increases in Marine Heatwave Duration

In this section, we focused on the remaining positive trend of marine heatwave duration after linear trend is removed (Figure 8a). As shown in Figure 10a, the two major components in the East Asian winter climate are the Siberian High (SH; Ding & Krishnamurti, 1987), which is the most robust cold-core high-pressure system ("H" in Figure 10a), and the Aleutian Low (AL; Jhun & Lee, 2004; Trenberth & Hurrell, 1994), which is a semi-permanent warm-core low-pressure system ("L" in Figure 10a).

In the earlier period (Figure 10b), the atmospheric variance on the western boundary of the AL tends to dominate the excessive increase in N-ES marine heatwave durations, revealing the negative effect of the AL (i.e., the increased SLP anomaly) on extending the detrended marine heatwave duration. In this process, a weakened AL results in a reduction of northerly winds and warm air transport from the tropical Pacific to East Asia, ultimately leading to an increase in SSTs (Figure 10a and Figure S3a in Supporting Information S1). However, this dominant large-scale atmospheric circulation impact has diminished in the recent period, and a higher-frequency, east-to-west wave-like SLP pattern appears (Figure 10c and Figure S3b in Supporting Information S1). We found that the SST pattern observed in the North Pacific Ocean exhibits a similar pattern to that of the negative Pacific Decadal Oscillation (PDO) in Figure S4 in Supporting Information S1.

The decreased influence of the AL on North Pacific (Figure 10b vs. Figure 10c) corresponds well with numerous previous studies (Fereday et al., 2020; Hwang et al., 2022; Litzow et al., 2020; Zhou et al., 2020; Zhuge & Tan, 2021). They mentioned that the eastward shift of the AL center is observed. Additionally, Zhuge and Tan (2021) explain why the increased impact of the zonal North Pacific Oscillation (Mode 3) is responsible for the east-to-west wave pattern (Figure S5 vs. Figure S6 in Supporting Information S1). As the North Pacific atmospheric circulation pattern has recently changed, the correlation between the N-ES marine heatwave duration and the western part of the AL index (160°E–160°W, 30°N–50°N, modified North Pacific index (Trenberth & Hurrell, 1994)) decreased from 0.41 (with a 90% confidence level) to 0.28 (not significant).

Instead, we suggest an increasing connection between the ocean current and the N-ES marine heatwave duration in the recent period. Wang et al. (2022) also suggested that the increase in marine heatwave in the East Sea region may be explained by ocean dynamics rather than atmospheric forcing. Figures 10d and 10e show the daily mean ocean current and standard deviation of the meridional current. Here, we propose that the variability of meridional current may indicate the north-south location of the extension of EKWC. For example, an increase of standard deviation in the N-ES as shown upper box of Figure 10e can denote that EKWC

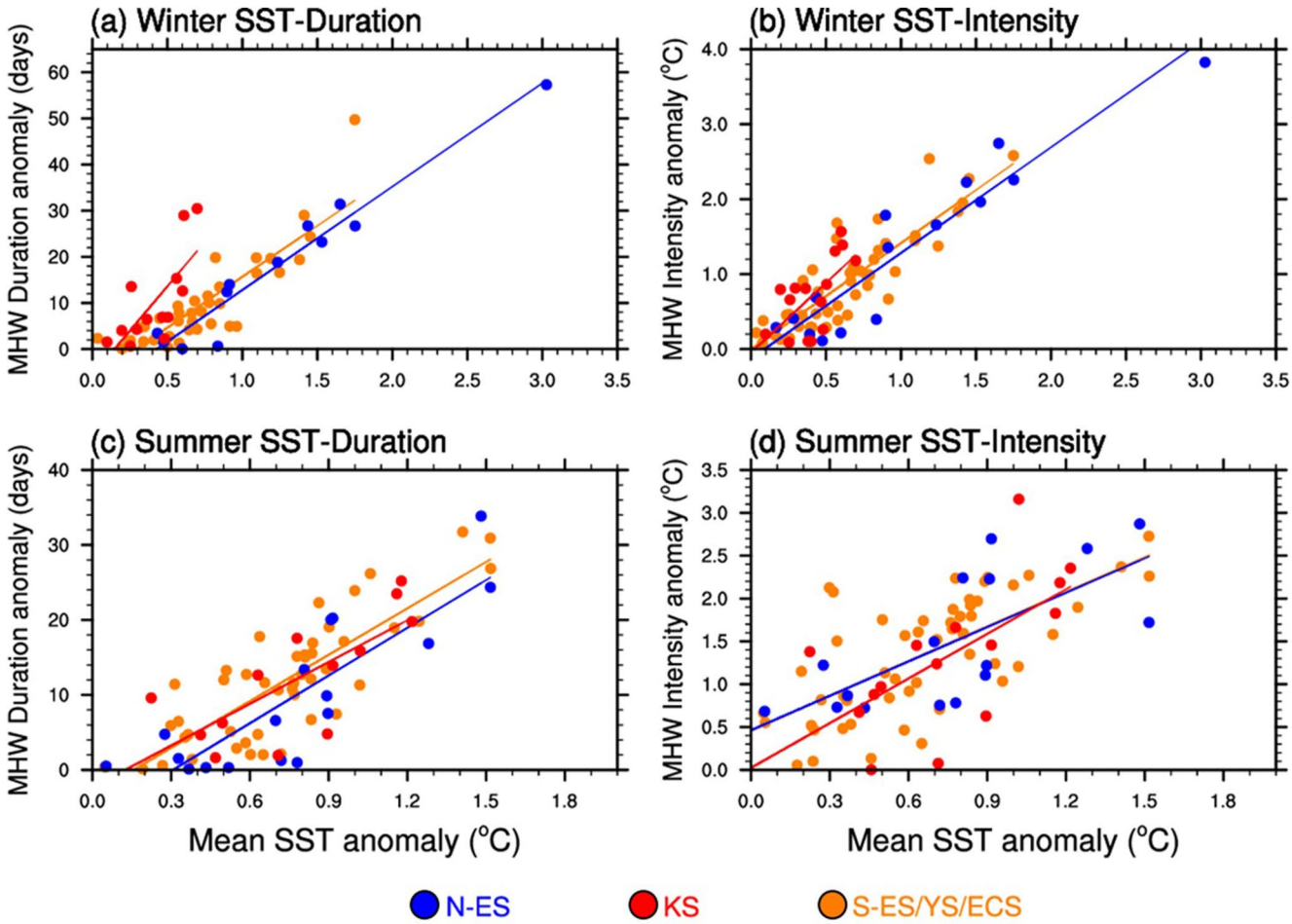

Figure 7. Scatter plot shows the relationship between regional averaged SST anomaly and marine heatwave characteristics anomalies including duration and intensity during winter (top panel) and summer (bottom panel). Blue (red) dots represent the marine heatwave characteristics of N-ES (KS) regions and orange dots represent the combined marine heatwave characteristics of S-ES, YS, and ECS regions.

reaches more northward in the recent period. The atmosphere and ocean processes affecting the winter N-ES marine heatwave duration during earlier period and recent period are shown in Figure 11. In the earlier period, the weakened AL dominantly influenced the N-ES marine heatwave events by transporting warm air from the south (Figure 11a). Recently, more northward-shifted EKWC anomalies (Figure S7 in Supporting Information S1) and increased meridional current variance can induce an increased SST variance than the earlier period, further increases in the marine heatwave duration variance (Figure 11b). Our suggested mechanism that an atmospheric influence predominated in the earlier period, but an oceanic influence increased SST variance in the recent period, is briefly summarized in Figure 11c. This mechanism is similar to that proposed by Choi et al. (2022), that the northward shift of the subpolar front drives the winter marine heatwaves over the East Sea. Pak et al. (2019) mentioned that the separation latitude of the EKWC has interannual variations and recently tends to shift northward, beyond 38°N. Previous studies (Cho & Kim, 1996; Choi et al., 2018; Hogan & Hurlburt, 2000; Marshall & Tansley, 2001; Pak et al., 2019; Yoon et al., 2016) have noted that it is not clear what mechanisms influence the variability of meridian motion in EKWC. The variability in the meridional EKWC may be influenced by the increased ocean temperature condition (Pak et al., 2019) or heat content anomaly (Yoon et al., 2016). In addition, ocean circulation can modify the vertical stability as well as the horizontal heat distribution of the upper ocean (Pai et al., 2023). Further study is necessary to clarify how the three-dimensional ocean circulation affects marine heatwave.

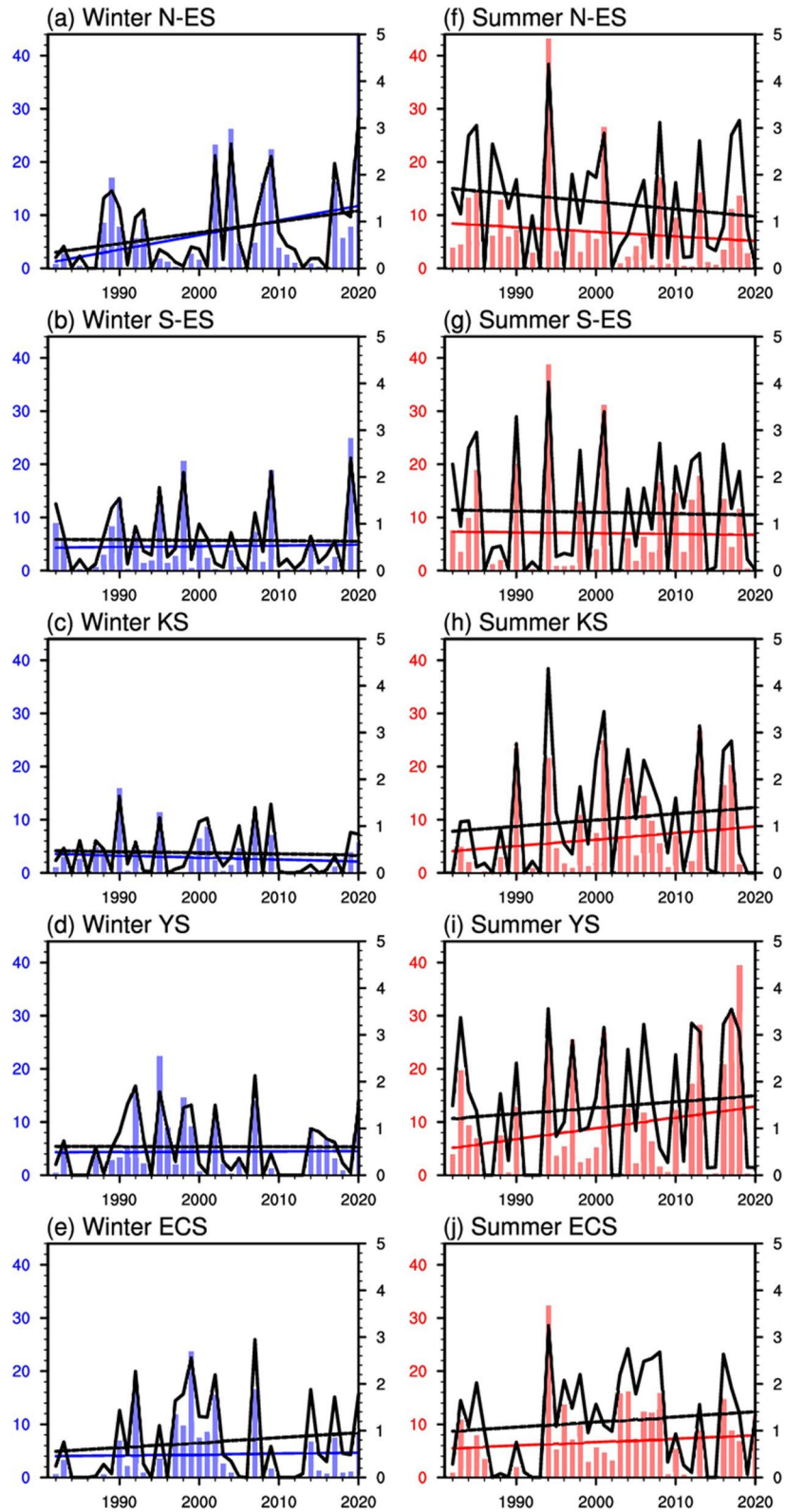

Figure 8. Same as Figure 5 but detecting marine heatwaves by detrended daily SST.

Table 4
Trend of Marine Heatwave Duration (Unit: days decade^{-1}) and Intensity (Unit: °C decade^{-1}) Detected Using Original SST and Detrended SST

	Original SST		Detrended SST	
	Duration days/decade	Intensity °C/decade	Duration days/decade	Intensity °C/decade
Winter				
Northern ES	**6.15****	**0.54****	**2.75***	**0.23***
Southern ES	**4.14****	**0.32****	0.14	−0.01
Korea Strait	**3.38****	**0.21****	−0.37	−0.02
Yellow Sea	0.17	0.01	0.05	−0.00
East China Sea	**2.65****	**0.38****	0.18	0.11
Summer				
Northern ES	**2.90****	**0.43****	−0.86	−0.16
Southern ES	1.41	0.18	−0.16	−0.03
Korea Strait	**2.34***	0.26	1.21	0.13
Yellow Sea	2.19	0.18	2.04	0.13
East China Sea	**4.48****	**0.59****	0.64	0.11

Note. Bold numerical values are significant with a 90% (*) and 95% (**) confidence level.

5. Summary and Conclusion

This study highlights that in a warming climate state, the EAMS are fast-changing seas due to multiple atmospheric and ocean circulation changes adjacent to the world's largest continent and largest ocean basin. In particular, the EAMS are threatened with more heat stress than the global average (Belkin, 2009; Clift et al., 2003; Wu et al., 2012). The main goals of this study are to quantify the long-term trends in marine heatwave properties in the EAMS and to examine the physical drivers responsible for any noticeable trend.

First, we find rapidly changing marine heatwave duration and intensity in the EAMS compared to the global average change. Overall, the increase in winter SST occurs in most of the EAMS, except along the western coastline of Korea. The most rapidly warming regions are the East Sea, the ECS, and the passages of the Kuroshio current (>0.3°C decade^{-1} for the last 39 years). Here, marine heatwave days and intensity have increased significantly by approximately +4 days and +0.3°C decade^{-1}, respectively (Figures 4b and 4c; Table 2). In particular, we highlight the remarkable rapidly increasing trends in the N-ES, finding 763.33% longer marine heatwaves with 320.08% stronger intensity in the recent two decades (2001–2020) than in the earlier period (1982–2000). In summer, the SST trends are not statistically significant, especially in the coastal seas around Korea. Despite the lack of significant change in mean SST, the KS reveals notable increasing trends in the summer marine heatwave properties, revealing approximately 135.69% longer durations with 68.76% stronger intensity in the recent two decades than in the earlier period.

In general, the rapidly increasing mean SST trend primarily results in the positive trends of marine heatwave properties in most regions of the EAMS (Figure 3). Correspondingly, we confirm the linear relationship between mean SSTs and East Asian marine heatwave properties (Section 4.1). In the recalculated marine heatwave trends with the detrended daily SST, the increasing trends disappear in most regions. However, we also find an excessive positive trend in winter marine heatwaves over the N-ES even after the removal of the mean trend (Figure 8a). This result indicates that other regional factors, in addition to climatological ocean warming trends, contribute to leading the changing marine heatwave properties.

We investigate the physical reasons for more rapidly changing marine heatwaves in the N-ES and ECS in winter. This study reveals the change in major winter climate systems responsible for SST variance. The AL had a dominant impact during the earlier period; however, we find increasing variance in the ocean current rather than atmospheric forcing during the recent period (Figure 10). The larger variance where the EKWC moves northward can lead to increased SST variance (Section 4.2, Figures 10d and 10e, Figure 11).

The current results have critical implications for future changes in marine heatwaves. With continued global warming, some subocean regions (e.g., the East Sea) experiencing atmospheric variability, decadal changes in the climate index, and changes in ocean structure (possible factors in marine heatwaves) may undergo more dramatic changes in future marine heatwaves. In addition, marine heatwaves are well known to be more robust and more extended in future climates (Oliver et al., 2018; Plecha & Soares, 2020). We analyze the future marine heatwave changes using the Coupled Model Intercomparison Project Phase 6 (CMIP6) future scenario (especially extreme future scenario, socioeconomic pathways (SSPs) 5- Representative Concentration Pathways (RCP) 8.5). Multi-model ensemble mean shows that in 2050, total marine heatwave duration will increase to approximately 64 and 88 days in winter and summer, respectively (Figure 12). These are substantial changes, considering that the current total marine heatwave durations are less than 8 days in winter and 7–9 days in summer (Table 1). These four models for marine heatwave characteristics had the same increasing trend in the future scenario, but the variability was relatively large. We plan to conduct variability studies for future marine heatwave characteristics using more CMIP6 models in future studies.

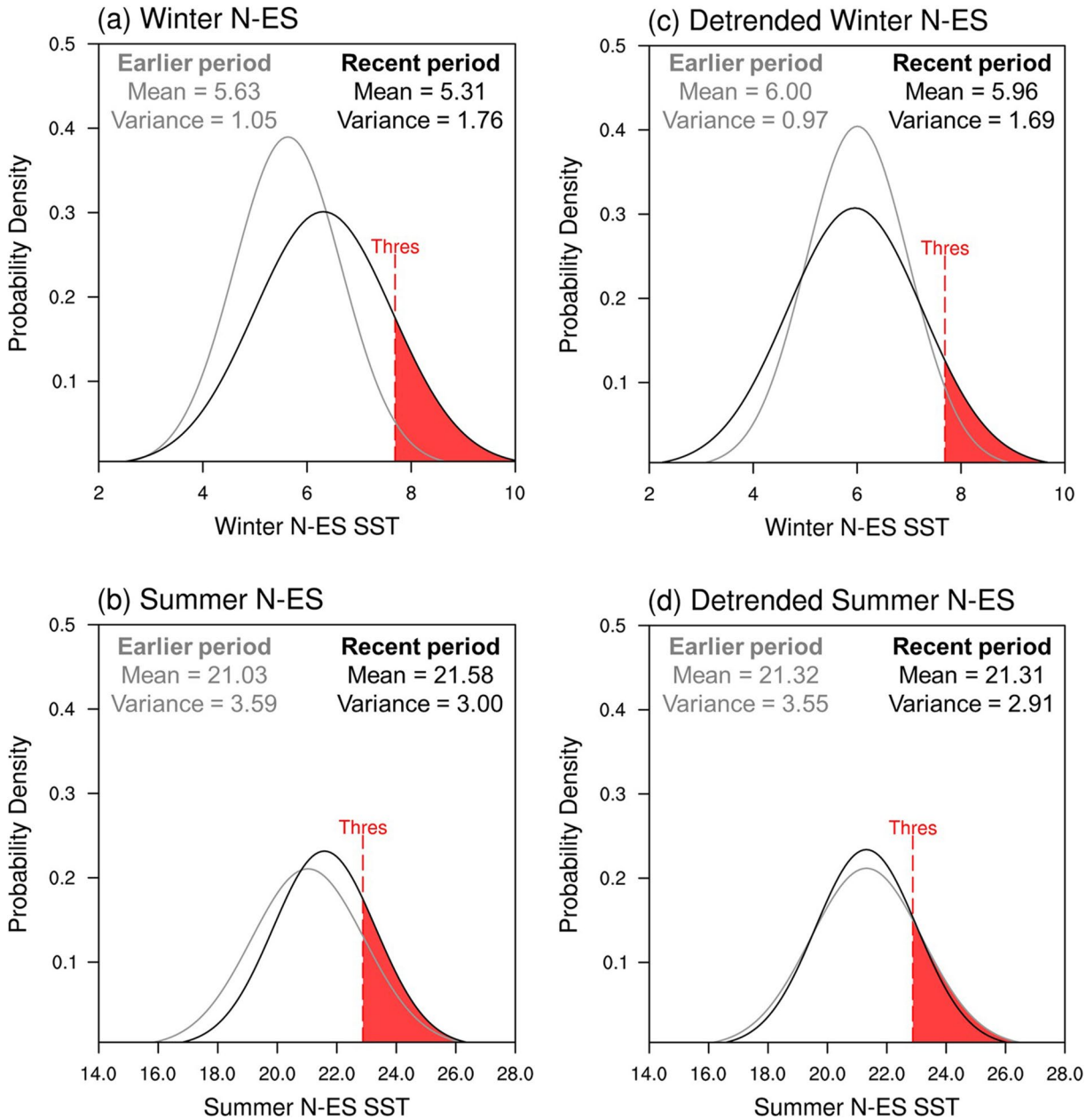

Figure 9. Probability distribution function for the averaged N-ES SST during winter (top panel) and summer (bottom panel). The gray line indicates for the earlier period (1982–2000) and black line represents for the recent period (2001–2020). The dashed red line means the threshold temperature of marine heatwave. The left (right) figures show before detrend (after detrend).

Such substantial changes in extreme ocean phenomena can have devastating impacts on the marine ecosystem in the EAMS. Effects already occurring include coral bleaching in the ES and near Jeju Island (Hwang et al., 2017; Yoo et al., 2016), a reduction in aquaculture production (KMI, 2020), and a shift in fish species (Kim et al., 2014) over the EAMS. To reduce the damage caused by marine heatwaves and to enable proactive decision-making, it is necessary to continuously observe ocean structure and circulation and further improve the scientific understanding of atmospheric factors related to marine heatwaves.

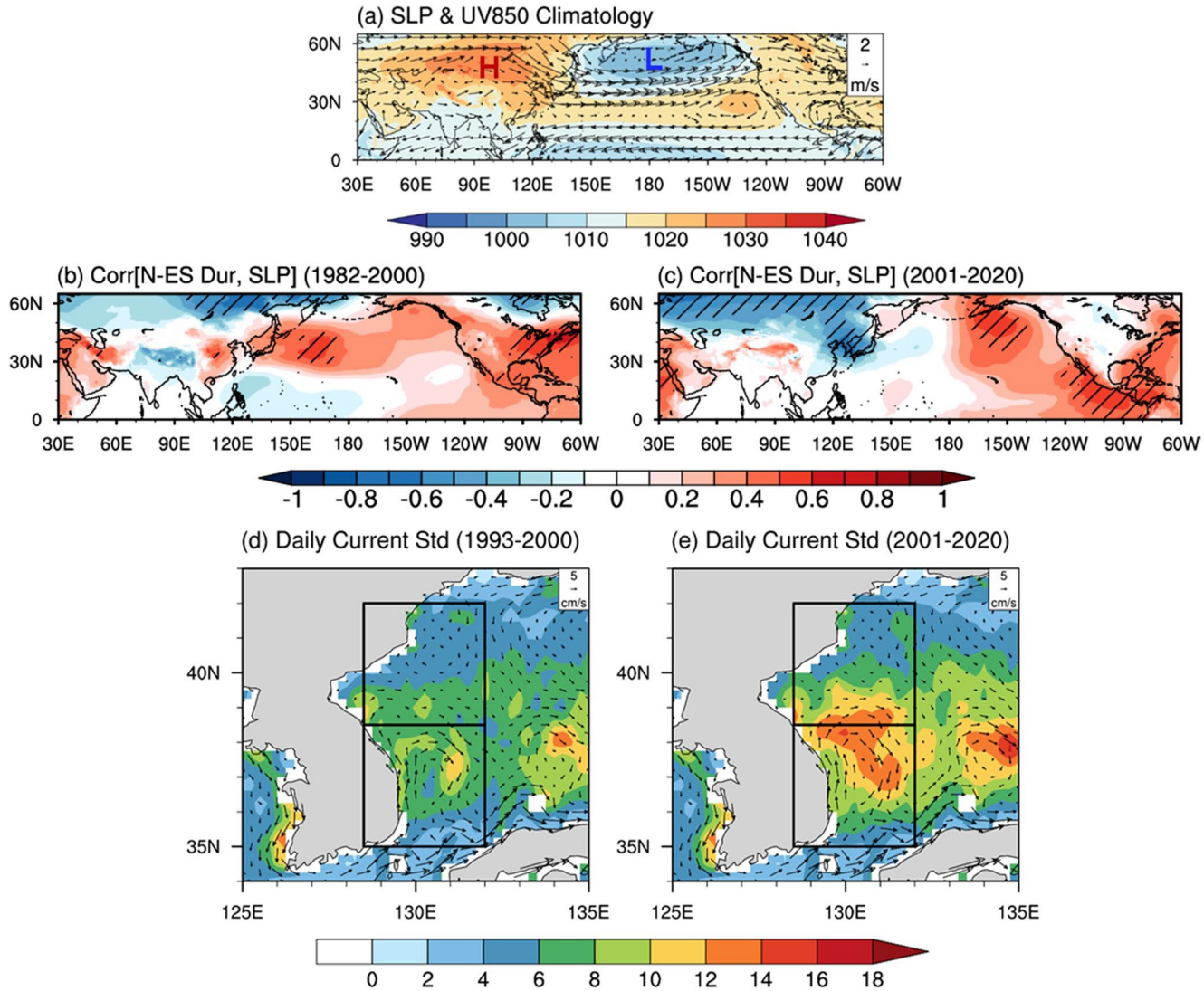

Figure 10. Winter mean of (a) sea level pressure (SLP, unit: hPa) and wind at 850 hPa (unit: m s^{-1}). Correlation map showing the correlation coefficient between detrended marine heatwave duration index over N-ES region and detrended anomalous sea level pressure during (b) earlier period (1982–2000) and (c) recent period (2001–2020) in winter using ERA5. Daily mean current (arrow, unit: cm s^{-1}) and standard deviation (contour, unit: cm s^{-1}) of detrended meridional ocean current during (d) earlier period (1993–2000) and (e) recent period (2001–2020) in winter.

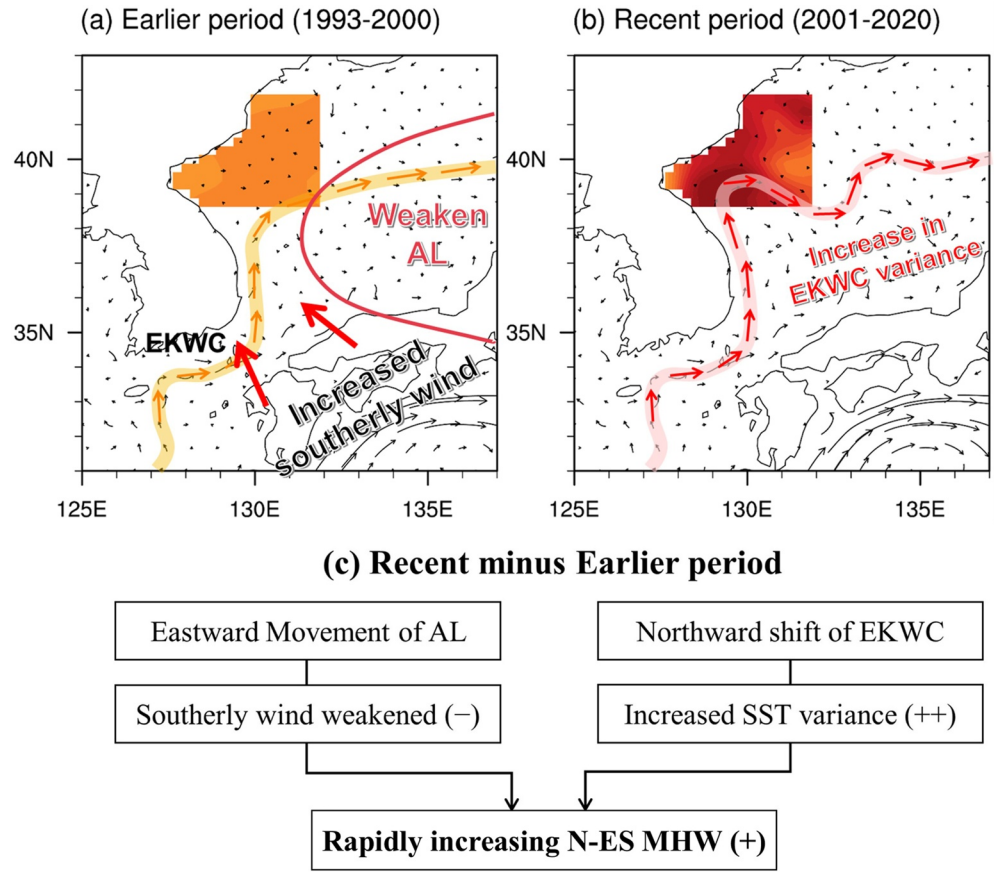

Figure 11. Schematic of the atmosphere and ocean processes affecting the winter N-ES marine heatwave duration during (a) earlier period, (b) recent period, and (c) difference between earlier and recent period. Orange arrows represent the EKWC during 1993–2000. Red circle (red arrows) indicates the anomalous anti-cyclonic circulation ((a) anomalous wind and (b) ocean current). Colored shades are shown as anomalous warm SST strength: The averaged SST in N-ES region is (a) 0.02°C and (b) 0.60°C.

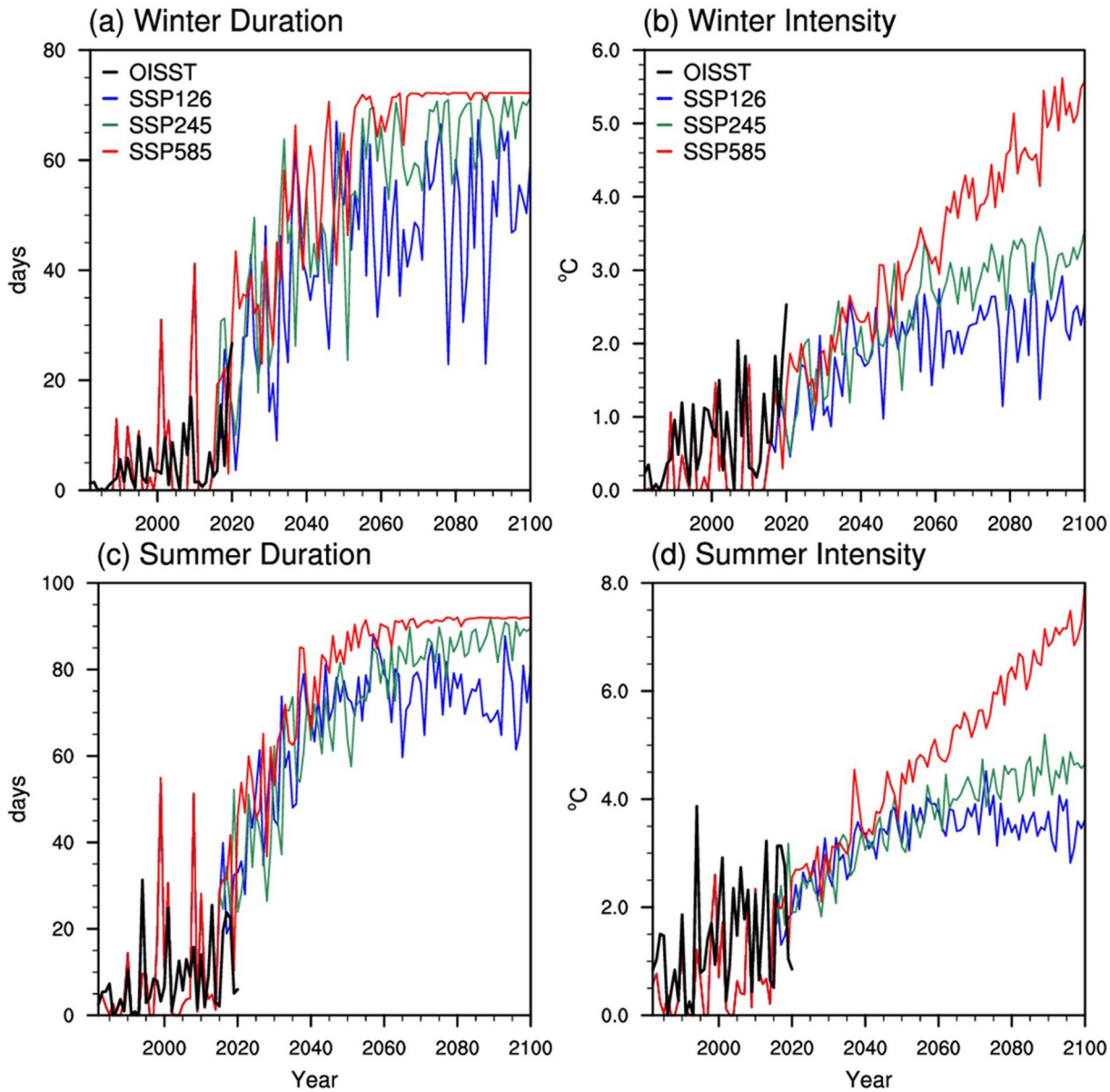

Figure 12. Time series of the marine heatwave characteristics during winter (a, b) and summer (c, d) over study regions under three socioeconomic pathways (SSPs) SSP1- Representative Concentration Pathways (RCP) 2.6 (blue line), SSP2-RCP 4.5 (green line), and SSP5-RCP8.5 (red line) from 1982 to 2100. The black lines represent the marine heatwave characteristics corresponding to OISST during 1982–2020. The marine heatwave characteristics value is the average of the five study regions based on the multi-model ensemble mean (BCC-CSM2-MR, CanESM5, CESM2-WACCM, and MIROC6).

Appendix A: Removing a Linear Trend of SST

The daily SST for 39 years follows a normal distribution with a mean value of μ and a variance of σ^2 (Pardo et al., 2017). A normal distribution can be converted to a standard normal distribution with a mean value of 0 and a variation in σ^2 (exactly 1^2). A warming climate results in an increase in SST as well as changes in the mean and variance. We consider two cases: increasing mean (but constant variance) and increasing variance (but constant mean). We proceed with the explanation of these two cases (Equations A1–A4) for a standard normal distribution with reference to Oliver (2019).

A1. Increasing Mean

We assume that SST_m=SST + mt, where m is a constant (subscript "m" of SST_m defines the change in mean). In this case, the mean and variance are given by

$$\mu_m = E[SST_m] = E[SST + mt] = E[SST] + mt = \mu + mt = mt \tag{A1}$$

$$\sigma_m^2 = E\left[(SST_m - \mu_m)^2\right] = E\left[(SST + mt - mt)^2\right] = E\left[SST^2\right] = \sigma^2 \tag{A2}$$

Here, the mean increases from 0 to mt, and the variance remains σ^2.

A2. Increasing Variance

We assume that $SST_v = SST\,(1 + vt)$, where v is a constant (subscript "v" of SST_v defines the change in variance). In this case, the mean and variance are given by

$$\mu_v = E[SST_v] = E[SST(1 + vt)] = E[SST + vtSST] = E[SST] + vtE[SST] = \mu + vt\mu = 0 \tag{A3}$$

$$\begin{aligned}\sigma_v^2 &= E\left[(SST_v - \mu_v)^2\right] = E\left[(SST + vtSST - 0)^2\right] = E\left[SST^2 + 2vtSST^2 + (vtSST)^2\right] \\ &= E\left[SST^2\right] + 2vtE\left[SST^2\right] + (vt)^2 E\left[SST^2\right] = \sigma^2 + 2vt\sigma^2 + (vt)^2\sigma^2 \\ &= \sigma^2\left(1 + 2vt + (vt)^2\right)\end{aligned} \tag{A4}$$

In this case, the variance increases from σ^2 to $\sigma^2\,(1 + 2vt + (vt)^2)$, and the mean remains 0. Under warming climate conditions, changes in the mean and variance of oceanic and atmospheric variables can influence extreme ocean events. To identify the role of the mean and variance changes in marine heatwaves, the effect of the mean change is analyzed by removing the mean ("detrending"), and the effect of variance is examined with the signal remaining after removing the mean.

A3. Detrending Mean

Detrending is the removal of the mean value or linear trend (least squares linear trend). In this study, we detrend to exclude the effect of a warming climate on SSTs and marine heatwaves. Through this method, the effect of the increasing mean is minimized, and the effect of the increasing variance is analyzed. Equation A5 indicates the linear trend of daily SST with the slope a and y-intercept b. At all grid points, the removed trend SST (detrended SST) is calculated by subtracting the linear trend from the original SST, as shown in Equation A6.

$$\hat{SST} = aSST + b \tag{A5}$$

$$\tilde{SST}_d = SST - \hat{SST} \tag{A6}$$

Data Availability Statement

Datasets that support the findings of this study are all openly available. The NOAA OISST daily data can be accessed at https://psl.noaa.gov/data/gridded/data.noaa.oisst.v2.highres.html, and the ERA5 data are provided https://cds.climate.copernicus.eu/cdsapp#!/dataset/reanalysis-era5-single-levels-monthly-means?tab=form. The GLORYS data is available at https://data.marine.copernicus.eu/product/GLOBAL_MULTIYEAR_PHY_001_030/services. The CMIP6 model output is publicly accessed at https://esgf-node.llnl.gov/search/cmip6/.

Acknowledgments
This research was a part of the project titled "Investigation and prediction system development of marine heatwave around the Korean Peninsula originated from the subarctic and western Pacific (20190344)," funded by the Ministry of Oceans and Fisheries, Korea.

References

Amaya, D. J., Miller, A. J., Xie, S. P., & Kosaka, Y. (2020). Physical drivers of the summer 2019 North Pacific marine heatwave. *Nature Communications*, *11*(1), 1–9. https://doi.org/10.1038/s41467-020-15820-w

Bao, B., & Ren, G. (2014). Climatological characteristics and long-term change of SST over the marginal seas of China. *Continental Shelf Research*, *77*, 96–106. https://doi.org/10.1016/j.csr.2014.01.013

Belkin, I. M. (2009). Rapid warming of large marine ecosystems. *Progress in Oceanography*, *81*(1–4), 207–213. https://doi.org/10.1016/j.pocean.2009.04.011

Cho, Y. K., & Kim, K. (1996). Seasonal variation of the East Korea Warm Current and its relation with the cold water. *La mer*, *34*, 172–182.

Choi, B. J., Cho, S. H., Jung, H. S., Lee, S. H., Byun, D. S., & Kwon, K. (2018). Interannual variation of surface circulation in the Japan/East Sea due to external forcings and intrinsic variability. *Ocean Science Journal*, *53*(1), 1–16. https://doi.org/10.1007/s12601-017-0058-8

Choi, N., & Lee, M. I. (2019). Spatial variability and long-term trend in the occurrence frequency of heatwave and tropical night in Korea. *Asia-Pacific Journal of Atmospheric Sciences*, *55*(1), 101–114. https://doi.org/10.1007/s13143-018-00101-w

Choi, N., Lee, M. I., Cha, D. H., Lim, Y. K., & Kim, K. M. (2020). Decadal changes in the interannual variability of heat waves in East Asia caused by atmospheric teleconnection changes. *Journal of Climate*, *33*(4), 1505–1522. https://doi.org/10.1175/jcli-d-19-0222.1

Choi, W., Bang, M., Joh, Y., Ham, Y. G., Kang, N., & Jang, C. J. (2022). Characteristics and mechanisms of marine heatwaves in the East Asian marginal seas: Regional and seasonal differences. *Remote Sensing*, *14*(15), 3522. https://doi.org/10.3390/rs14153522

Clark, N. J., Kerry, J. T., & Fraser, C. I. (2020). Rapid winter warming could disrupt coastal marine fish community structure. *Nature Climate Change*, *10*(9), 862–867. https://doi.org/10.1038/s41558-020-0838-5

Clift, P. D., Wang, P., Kuhnt, W., Hall, R., & Tada, R. (2003). Continent-ocean interactions within the East Asian marginal seas. *Eos, Transactions American Geophysical Union*, *84*(15), 139–141. https://doi.org/10.1029/2003eo150005

Cohen, J., Screen, J. A., Furtado, J. C., Barlow, M., Whittleston, D., Coumou, D., et al. (2014). Recent Arctic amplification and extreme mid-latitude weather. *Nature Geoscience*, *7*(9), 627–637. https://doi.org/10.1038/ngeo2234

Ding, Y., & Krishnamurti, T. N. (1987). Heat budget of the Siberian high and the winter monsoon. *Monthly Weather Review*, *115*(10), 2428–2449. https://doi.org/10.1175/1520-0493(1987)115<2428:hbotsh>2.0.co;2

Feng, M., McPhaden, M. J., Xie, S. P., & Hafner, J. (2013). La Niña forces unprecedented Leeuwin current warming in 2011. *Scientific Reports*, *3*(1), 1277. https://doi.org/10.1038/srep01277

Fereday, D. R., Chadwick, R., Knight, J. R., & Scaife, A. A. (2020). Tropical rainfall linked to stronger future ENSO-NAO teleconnection in CMIP5 models. *Geophysical Research Letters*, *47*(22), e2020GL088664. https://doi.org/10.1029/2020gl088664

Fischer, E. M., Seneviratne, S. I., Vidale, P. L., Lüthi, D., & Schär, C. (2007). Soil moisture–atmosphere interactions during the 2003 European summer heat wave. *Journal of Climate*, *20*(20), 5081–5099. https://doi.org/10.1175/jcli4288.1

Frölicher, T. L., & Laufkötter, C. (2018). Emerging risks from marine heat waves. *Nature Communications*, *9*(1), 650. https://doi.org/10.1038/s41467-018-03163-6

Gao, G., Marin, M., Feng, M., Yin, B., Yang, D., Feng, X., et al. (2020). Drivers of marine heatwaves in the East China Sea and the South Yellow Sea in three consecutive summers during 2016–2018. *Journal of Geophysical Research: Oceans*, *125*(8), e2020JC016518. https://doi.org/10.1029/2020jc016518

Garric, G., Parent, L., Greiner, E., Drévillon, M., Hamon, M., Lellouche, J. M., et al. (2018). Performance and quality assessment of the global ocean eddy-permitting physical reanalysis GLORYS2V4. In *Proceedings of the Eight EuroGOOS International Conference* (pp. 215–222). Retrieved form https://eurogoos.eu/download/eurogoos-2017-58/?wpdmdl=10118&refresh=647645df9e0aa1685472735

Han, I. S., & Lee, J. S. (2020). Change the annual amplitude of sea surface temperature due to climate change in a recent decade around the Korean Peninsula. *Journal of the Korean Society of Marine Environment and Safety*, *26*(3), 233–241. https://doi.org/10.7837/kosomes.2020.26.3.233

Hobday, A. J., Alexander, L. V., Perkins, S. E., Smale, D. A., Straub, S. C., Oliver, E. C. J., et al. (2016). A hierarchical approach to defining marine heatwaves. *Progress in Oceanography*, *141*, 227–238. https://doi.org/10.1016/j.pocean.2015.12.014

Hogan, P. J., & Hurlburt, H. E. (2000). Impact of upper ocean–topographical coupling and isopycnal outcropping in Japan/East Sea models with 1/8° to 1/64° Resolution. *Journal of Physical Oceanography*, *30*(10), 2535–2561. https://doi.org/10.1175/1520-0485(2000)030<2535:iouotc>2.0.co;2

Hughes, T. P., Kerry, J. T., Álvarez-Noriega, M., Álvarez-Romero, J. G., Anderson, K. D., Baird, A. H., et al. (2017). Global warming and recurrent mass bleaching of corals. *Nature*, *543*(7645), 373–377. https://doi.org/10.1038/nature21707

Hwang, S. I., Kim, D. K., Sung, B. J., Jun, S. K., Bae, J. I., & Jeon, B. H. (2017). Effects of climate change on whitening event proliferation the coast of Jeju. *Korean Journal of Environment and Ecology*, *31*(6), 529–536. https://doi.org/10.13047/kjee.2017.31.6.529

Hwang, S. O., Yeh, S. W., Oh, S. Y., & Lee, J. (2022). Recent weakening linkage between Arctic oscillation and Aleutian low during boreal winter and its impact on surface temperature over Eastern Eurasia. *Atmospheric Science Letters*, *23*(7), e1089. https://doi.org/10.1002/asl.1089

Jhun, J. G., & Lee, E. J. (2004). A new East Asian winter monsoon index and associated characteristics of the winter monsoon. *Journal of Climate*, *17*(4), 711–726. https://doi.org/10.1175/1520-0442(2004)017<0711:aneawm>2.0.co;2

Jung, H. K., Rahman, S. M., Kang, C. K., Park, S. Y., Lee, S. H., Park, H. J., et al. (2017). The influence of climate regime shifts on the marine environment and ecosystems in the East Asian Marginal Seas and their mechanisms. *Deep Sea Research Part II: Topical Studies in Oceanography*, *143*, 110–120. https://doi.org/10.1016/j.dsr2.2017.06.010

Kennedy, J. J. (2014). A review of uncertainty in in situ measurements and data sets of sea surface temperature. *Reviews of Geophysics*, *52*(1), 1–32. https://doi.org/10.1002/2013rg000434

Kim, D. W., Park, Y. J., Jeong, J. Y., & Jo, Y. H. (2020). Estimation of hourly sea surface salinity in the East China Sea using geostationary ocean color imager measurements. *Remote Sensing*, *12*(5), 755. https://doi.org/10.3390/rs12050755

Kim, S. J., Woo, S. H., Kim, B. M., & Hur, S. D. (2011). Trends in sea surface temperature (SST) change near the Korean peninsula for the past 130 years. *Ocean and Polar Research*, *33*(3), 281–290. https://doi.org/10.4217/opr.2011.33.3.281

Kim, T. S., Park, K. A., Li, X., & Hong, S. (2014). SAR-derived wind fields at the coastal region in the East/Japan sea and relation to coastal upwelling. *International Journal of Remote Sensing*, *35*(11–12), 3947–3965. https://doi.org/10.1080/01431161.2014.916438

KMI. (2020). Concerns about disruption of seaweed supply due to abnormally high temperature, need to reorganize supply and demand management system. *KMI Weekly Report*, *166*, 1–18. Retrieved from https://www.kmi.re.kr/web/logIn/web/trebook/view.do?rbsIdx=273&page=3&idx=184

Kug, J. S., Jeong, J. H., Jang, Y. S., Kim, B. M., Folland, C. K., Min, S. K., & Son, S. W. (2015). Two distinct influences of Arctic warming on cold winters over North America and East Asia. *Nature Geoscience*, *8*(10), 759–762. https://doi.org/10.1038/ngeo2517

Larsen, J. (2003). *Record heat wave in Europe takes 35,000 lives: Far greater losses may lie ahead*. Earth Policy Institute.

Lee, E. Y., & Park, K. A. (2020). Validation of satellite sea surface temperatures and long-term trends in Korean coastal regions over past decades (1982–2018). *Remote Sensing*, *12*(22), 3742. https://doi.org/10.3390/rs12223742

Lee, S., Park, M. S., Kwon, M., Kim, Y. H., & Park, Y. G. (2020). Two major modes of East Asian marine heatwaves. *Environmental Research Letters*, *15*(7), 074008. https://doi.org/10.1088/1748-9326/ab8527

Lee, W. S., & Lee, M. I. (2016). Interannual variability of heat waves in South Korea and their connection with large-scale atmospheric circulation patterns. *International Journal of Climatology*, *36*(15), 4815–4830. https://doi.org/10.1002/joc.4671

Lima, F. P., & Wethey, D. S. (2012). Three decades of high-resolution coastal sea surface temperatures reveal more than warming. *Nature Communications*, *3*(1), 1–13. https://doi.org/10.1038/ncomms1713

Litzow, M. A., Hunsicker, M. E., Bond, N. A., Burke, B. J., Cunningham, C. J., Gosselin, J. L., et al. (2020). The changing physical and ecological meanings of North Pacific Ocean climate indices. *Proceedings of the National Academy of Sciences of the United States of America*, *117*(14), 7665–7671. https://doi.org/10.1073/pnas.1921266117

Marshall, D. P., & Tansley, C. E. (2001). An implicit formula for boundary current separation. *Journal of Physical Oceanography*, *31*(6), 1633–1638. https://doi.org/10.1175/1520-0485(2001)031<1633:aiffbc>2.0.co;2

Masson-Delmotte, V., Zhai, P., Pirani, A., Connors, S. L., Péan, C., Berger, S., et al. (2021). Climate change 2021: The physical science basis. Contribution of working group I to the sixth assessment report of the intergovernmental panel on climate change (Vol. *2*).

Meehl, G. A., Stocker, T. F., Collins, W. D., Friedlingstein, P., Gaye, A. T., Gregory, J. M., et al. (2007). Global climate projections. Chapter 10.

Moon, J. H., Kim, T., Son, Y. B., Hong, J. S., Lee, J. H., Chang, P. H., & Kim, S. K. (2019). Contribution of low-salinity water to sea surface warming of the East China Sea in the summer of 2016. *Progress in Oceanography*, *175*, 68–80. https://doi.org/10.1016/j.pocean.2019.03.012

Noh, E., Kim, J., Jun, S.-Y., Cha, D.-H., Park, M.-S., Kim, J.-H., & Kim, H.-G. (2021). The role of the Pacific-Japan pattern in extreme heatwaves over Korea and Japan. *Geophysical Research Letters*, *48*(18), e2021GL093990. https://doi.org/10.1029/2021GL093990

Olita, A., Sorgente, R., Natale, S., Gaberšek, S., Ribotti, A., Bonanno, A., & Patti, B. (2007). Effects of the 2003 European heatwave on the Central Mediterranean sea: Surface fluxes and the dynamical response. *Ocean Science*, *3*(2), 273–289. https://doi.org/10.5194/os-3-273-2007

Oliver, E. C. J. (2019). Mean warming not variability drives marine heatwave trends. *Climate Dynamics*, *53*(3–4), 1653–1659. https://doi.org/10.1007/s00382-019-04707-2

Oliver, E. C. J., Benthuysen, J. A., Bindoff, N. L., Hobday, A. J., Holbrook, N. J., Mundy, C. N., & Perkins-Kirkpatrick, S. E. (2017). The unprecedented 2015/16 Tasman sea marine heatwave. *Nature Communications*, *8*, 1–12. https://doi.org/10.1038/ncomms16101

Oliver, E. C. J., Donat, M. G., Burrows, M. T., Moore, P. J., Smale, D. A., Alexander, L. V., et al. (2018). Longer and more frequent marine heatwaves over the past century. *Nature Communications*, *9*(1), 1–12. https://doi.org/10.1038/s41467-018-03732-9

Pai, R. U., Parekh, A., Chowdary, J. S., & Gnanaseelan, C. (2023). The interannual variability of shallow meridional overturning circulation and its association with the south-west Indian Ocean heat content variability. *Theoretical and Applied Climatology*, *151*(3), 1079–1094. https://doi.org/10.1007/s00704-022-04319-7

Pak, G., Kim, Y. H., & Park, Y. G. (2019). Lagrangian approach for a new separation index of the East Korea warm current. *Ocean Science Journal*, *54*(1), 29–38. https://doi.org/10.1007/s12601-018-0059-2

Pardo, D., Jenouvrier, S., Weimerskirch, H., & Barbraud, C. (2017). Effect of extreme sea surface temperature events on the demography of an age-structured albatross population. *Philosophical Transactions of the Royal Society of London. Series B, Biological Sciences*, *372*(1723), 20160143. https://doi.org/10.1098/rstb.2016.0143

Park, C. K., & Schubert, S. D. (1997). On the nature of the 1994 East Asian summer drought. *Journal of Climate*, *10*(5), 1056–1070. https://doi.org/10.1175/1520-0442(1997)010<1056:otnote>2.0.co;2

Park, K. A., & Kim, K. R. (2010). Unprecedented coastal upwelling in the East/Japan Sea and linkage to long-term large-scale variations. *Geophysical Research Letters*, *37*(9), L06609. https://doi.org/10.1029/2009gl042231

Park, K. A., Lee, E. Y., Chang, E., & Hong, S. (2015). Spatial and temporal variability of sea surface temperature and warming trends in the Yellow Sea. *Journal of Marine Systems*, *143*, 24–38. https://doi.org/10.1016/j.jmarsys.2014.10.013

Plecha, S. M., & Soares, P. M. (2020). Global marine heatwave events using the new CMIP6 multi-model ensemble: From shortcomings in present climate to future projections. *Environmental Research Letters*, *15*(12), 124058. https://doi.org/10.1088/1748-9326/abc847/meta

Rahman, S. M., Jung, H. K., Park, H. J., Park, J. M., & Lee, C. I. (2019). Synchronicity of climate driven regime shifts among the East Asian marginal sea waters and major fish species. *Journal of Environmental Biology*, *40*(5(SI)), 948–961. https://doi.org/10.22438/jeb/40/5(si)/si-18

Reynolds, R. W., Smith, T. M., Liu, C., Chelton, D. B., Casey, K. S., & Schlax, M. G. (2007). Daily high-resolution-blended analyses for sea surface temperature. [Dataset]. Journal of Climate, *20*(22), 5473–5496. https://doi.org/10.1175/2007jcli1824.1

Sasaki, Y. N., & Umeda, C. (2021). Rapid warming of sea surface temperature along the Kuroshio and the China coast in the East China Sea during the twentieth century. *Journal of Climate*, *34*(12), 4803–4815. https://doi.org/10.1175/jcli-d-20-0421.1

Simmons, A., Soci, C., Nicolas, J., Bell, B., Berrisford, P., Dragani, R., et al. (2020). Global stratospheric temperature bias and other stratospheric aspects of ERA5 and ERA5. 1. [Dataset]. https://doi.org/10.21957/rcxqfmg0

Stocker, T. F., Qin, D., Plattner, G. K., Tignor, M. M., Allen, S. K., Boschung, J., et al. (2014). Climate Change 2013: The physical science basis. contribution of working group I to the fifth assessment report of IPCC the intergovernmental panel on climate change.

Stott, P. A., Christidis, N., Otto, F. E. L., Sun, Y., Vanderlinden, J. P., van Oldenborgh, G. J., et al. (2016). Attribution of extreme weather and climate-related events. *Wiley Interdisciplinary Reviews: Climate Change*, *7*(1), 23–41. https://doi.org/10.1002/wcc.380

Trenberth, K. E., & Hurrell, J. W. (1994). Decadal atmosphere-ocean variations in the Pacific. *Climate Dynamics*, *9*(6), 303–319. https://doi.org/10.1007/bf00204745

Wang, B. (2006). *The Asian monsoon*. Springer Science & Business Media.

Wang, D., Xu, T., Fang, G., Jiang, S., Wang, G., Wei, Z., & Wang, Y. (2022). Characteristics of marine heatwaves in the Japan/East Sea. *Remote Sensing*, *14*(4), 936. https://doi.org/10.3390/rs14040936

Wang, Y. L., Wu, C. R., & Chao, S. Y. (2016). Warming and weakening trends of the Kuroshio during 1993-2013. *Geophysical Research Letters*, *43*(17), 9200–9207. https://doi.org/10.1002/2016gl069432

Wernberg, T., Bennett, S., Babcock, R. C., de Bettignies, T., Cure, K., Depczynski, M., et al. (2016). Climate-driven regime shift of a temperate marine ecosystem. *Science*, *353*(6295), 169–172. https://doi.org/10.1126/science.aad8745

Wernberg, T., Smale, D. A., Tuya, F., Thomsen, M. S., Langlois, T. J., de Bettignies, T., et al. (2013). An extreme climatic event alters marine ecosystem structure in a global biodiversity hotspot. *Nature Climate Change*, *3*(1), 78–82. https://doi.org/10.1038/nclimate1627

Wijffels, S., Roemmich, D., Monselesan, D., Church, J., & Gilson, J. (2016). Ocean temperatures chronicle the ongoing warming of Earth. *Nature Climate Change*, *6*(2), 116–118. https://doi.org/10.1038/nclimate2924

Wu, L., Cai, W., Zhang, L., Nakamura, H., Timmermann, A., Joyce, T., et al. (2012). Enhanced warming over the global subtropical Western boundary currents. *Nature Climate Change*, *2*(3), 161–166. https://doi.org/10.1038/nclimate1353

Yao, Y., Wang, J., Yin, J., & Zou, X. (2020). Marine heatwaves in China's marginal seas and adjacent offshore waters: Past, present, and future. *Journal of Geophysical Research: Oceans*, *125*(3), e2019JC015801. https://doi.org/10.1029/2019jc015801

Yoo, H. M., Park, J. Y., Song, Y. S., Lee, E. J., Kang, S. Y., Kim, J. H., et al. (2016). A study on coralline flat phenomenon of Korea. *The Journal of Applied Geography*, *33*, 79–102.

Yoon, S. T., Chang, K. I., Na, H., & Minobe, S. (2016). An east-west contrast of upper ocean heat content variation south of the subpolar front in the East/Japan Sea. *Journal of Geophysical Research: Oceans*, *121*(8), 6418–6443. https://doi.org/10.1002/2016jc011891

Zhou, W., Yang, D., Xie, S. P., & Ma, J. (2020). Amplified Madden–Julian oscillation impacts in the Pacific–North America region. *Nature Climate Change*, *10*(7), 654–660. https://doi.org/10.1038/s41558-020-0814-0

Zhuge, A., & Tan, B. (2021). The zonal North Pacific oscillation: A high-impact atmospheric teleconnection pattern influencing the North Pacific and North America. *Environmental Research Letters*, *16*(7), 074007. https://doi.org/10.1088/1748-9326/ac037b